Available online at www.sciencedirect.com
SCIENCE DIRECT®
International Journal of Mass Spectrometry 228 (2003) 599–611
International Journal of Mass Spectrometry
www.elsevier.com/locate/ijms

Catalytic gas phase dehydration of acetic acid to ketene

Tom Waters, Richard A.J. O'Hair*, Anthony G. Wedd

School of Chemistry, The University of Melbourne, Parkville, Vic. 3010, Australia

Received 25 February 2003; accepted 19 March 2003

Dedicated to Professor Helmut Schwarz on the occasion of his 60th birthday and in recognition of his many important contributions to organic, inorganic and organometallic chemistry.

Abstract

A two step gas phase catalytic cycle for the dehydration of acetic acid to ketene was detected by multistage mass spectrometry experiments. The catalysts are Group VI mononuclear $[MO_3(OH)]^-$ and binuclear $[M_2O_6(OH)]^-$ oxo-anions (M = Mo, W), formed via electrospray ionization. These catalytic cycles proceed via: (i) initial condensation of acetic acid to form $[MO_3(OCOCH_3)]^-$ or $[M_2O_6(OCOCH_3)]^-$, respectively, with elimination of water; and (ii) collisional activation of $[MO_3(OCOCH_3)]^-$ or $[M_2O_6(OCOCH_3)]^-$ to eliminate ketene, CH_2CO, and reform $[MO_3(OH)]^-$ or $[M_2O_6(OH)]^-$, respectively. In contrast to the molybdenum and tungsten congeners, the analogous chromium systems are unreactive towards acetic acid in the gas phase. The chromium acetate complexes (formed by adding trace amounts of acetic acid to the electrospray solution) undergo a variety of different fragmentation reactions, with a considerable reduction in selectivity towards ketene compared with the molybdenum and tungsten congeners. The reactivity of various oxo-anions was quantified by examining the kinetics for condensation reactions as well as the kinetic isotope effect and threshold activation energy for ketene elimination.
© 2003 Elsevier Science B.V. All rights reserved.

Keywords: Ketene; Gas phase; Tandem mass spectrometry; Catalysis; Dimolybdate

1. Introduction

Ketene ($H_2C{=}C{=}O$) is the parent member of a series of reactive species of general formula $RR'C{=}C{=}O$. The major industrial use of ketene is in the production of either acetic anhydride or diketene (via controlled dimerisation) [1]. Ketenes are also used in the preparation of β-lactones and β-lactams via [2+2] cycloaddition reactions with ketones and imines, respectively [2]. Current industrial production of ketene involves the pyrolysis of carboxylic acids or ketones at 740–760 °C (Eq. (1)) [1]. However, this reaction has a significant activation energy (65–73 kcal/mol) and is also in competition with decarboxylation (Eq. (2)) [3]. For these reasons, a catalytic process for the production of ketene from acetic acid that decreases the activation energy, while increasing the selectivity towards ketene, is highly desirable.

$$CH_3COOH \rightarrow CH_2CO + H_2O \quad (1)$$

$$CH_3COOH \rightarrow CO_2{+}CH_4 \quad (2)$$

A number of reports have appeared on the preparation of ketenes via the catalytic dehydration of carboxylic acids over silica, metal or metal-oxide surfaces [4]. These reactions are proposed to occur via two steps: (i) interaction of the parent carboxylic acid

* Corresponding author. Tel.: +61-3-8344-6490; fax: +61-3-8347-5180.
E-mail address: rohair@unimelb.edu.au (R.A.J. O'Hair).

1387-3806/$ – see front matter © 2003 Elsevier Science B.V. All rights reserved.
doi:10.1016/S1387-3806(03)00203-3

with a surface hydroxyl site to form a surface carboxylate with elimination of water (Eq. (3)); and (ii) decomposition of the surface carboxylate at elevated temperatures to liberate ketene and regenerate the surface hydroxyl site (Eq. (4)).

$$CH_3COOH + M\text{–}OH(ads) \rightarrow M\text{–}OCOCH_3(ads) + H_2O \quad (3)$$

$$M\text{–}OCOCH_3(ads) \rightarrow M\text{–}OH(ads) + H_2C{=}C{=}O \quad (4)$$

In order to gain insights into the fundamental interactions between metal ions and organic substrates, several groups have used sophisticated mass spectrometry techniques to examine the gas phase reactions of metal ions and their complexes [5]. There are a few reports only on the reactions of carboxylic acids with metal ions in the gas phase, with metal cations undergoing a variety of different reactions. For example, Co^+ inserted into the C–OH (predominantly) or the C–CO bond as the first step [6a], Fe^+ induced a number of reactions with decarbonylation dominating for smaller carboxylic acids [6b,6c], while Cu^+ reacted with acetic acid via dehydration (Eqs. (5) and (6)) [6d].

$$Cu^+ + CH_3COOH \rightarrow Cu(CH_2CO)^+ + H_2O \quad (5)$$

$$Cu^+ + CH_3COOH \rightarrow Cu(H_2O)^+ + CH_2CO \quad (6)$$

It is apparent that multistage mass spectrometry experiments can provide insights into the key reactions and intermediates in condensed phase catalytic processes [7]. Indeed, a number of gas phase catalytic cycles have been established previously [8], including pioneering work by Schwarz and co-workers on the catalytic oxidation of typically ‘inert’ and challenging substrates such as methane [9].

We have recently shown that the protonated dimolybdate anion $[Mo_2O_6(OH)]^-$ catalyses the gas phase oxidation of methanol to formaldehyde [10]. Similarities between this gas phase catalysis (Eq. (7)) and that occurring in the industrial oxidation of methanol to formaldehyde over solid state molybdenum(VI) oxide catalysts (Eq. (8)) were noted [10].

$$CH_3OH + CH_3NO_2 \rightarrow H_2CO + H_2O + CH_3NO \quad (7)$$

$$CH_3OH + 1/2O_2 \rightarrow H_2CO + H_2O \quad (8)$$

This gas phase catalysis proceeds via three steps: (1) reaction of $[Mo_2O_6(OH)]^-$ with alcohol and elimination of water to form $[Mo_2O_6(OCHR_2)]^-$; (2) oxidation of the alkoxo ligand and its elimination as aldehyde in the rate-determining step; and (3) regeneration of the catalyst via oxidation by nitromethane. Two important similarities between this gas phase catalysis and that proposed for the formation of ketene over metal oxide surfaces (Eqs. (3) and (4)) are apparent. Firstly, the reaction between $[Mo_2O_6(OH)]^-$ and alcohol is a condensation reaction similar to that shown in (Eq. (3)) for the interaction between CH_3COOH and an M–OH unit at a metal-oxide surface. Secondly, the elimination of aldehyde from $[Mo_2O_6(OR)]^-$ centers can potentially be in competition with the non-redox elimination of alkene, a reaction similar to that required for the elimination of ketene from $M\text{–}OCOCH_3$ units (Eq. (4)). Indeed, we have shown that this alkene elimination reaction could be “switched on” either by altering the alkoxo ligand to one without an α-hydrogen (e.g., collisional activation of $[Mo_2O_6(OC(CH_3)_3)]^-$ resulted in the non-redox elimination of 2-methylpropene, Eq. (9)) or by changing the metal-oxo anion to one that is a weaker oxidant, e.g., $[W_2O_6(OCHR_2)]^-$ preferred the non-redox elimination of alkene over aldehyde, even when an α-hydrogen was present in the alkoxo ligand (Eq. (10)).

$$[Mo_2O_6(OC(CH_3))_3]^- \rightarrow [Mo_2O_6(OH)]^- + (CH_3)_2C{=}CH_2 \quad (9)$$

$$[W_2O_6(OCH_2CH_3)]^- \rightarrow [W_2O_6(OH)]^- + CH_2{=}CH_2 \quad (10)$$

The product of alkene elimination was $[M_2O_6(OH)]^-$ (M = Mo, W; Eqs. (9) and (10)). This ion could further react with alcohol ROH to eliminate water and regenerate $[M_2O_6(OR)]^-$. These two reactions result in a simple gas phase catalytic cycle for the dehydration of alcohols to alkenes. In this paper, we describe a related two-step gas phase catalytic cycle for the dehydration of acetic acid to ketene using the oxo-anions $[MO_3(OH)]^-$ or $[M_2O_6(OH)]^-$ as catalysts (M = Mo, W). The two steps of this gas

phase catalysis are related to those proposed to occur on silica or metal oxide surfaces in the condensed phase (Eqs. (3) and (4)) [4].

2. Experimental

2.1. Synthesis

Tetra-*n*-butylammonium (Bu_4N^+) salts of $[Cr_2O_7]^{2-}$, $[Mo_2O_7]^{2-}$, $[CrO_4]^{2-}$, $[MoO_4]^{2-}$, and $[WO_4]^{2-}$ were synthesized using standard literature methods [11–15].

2.2. Reagents

Acetic acid (HPLC grade, 99.8%) was obtained from Aldrich and used without further purification. Acetonitrile (HPLC grade, 99.8%) was obtained from Merck. CH_3CHDCO_2H was synthesised using a standard literature procedure [16]. The position of the deuterium was confirmed using proton decoupled ^{13}C NMR, while the deuterium incorporation was estimated to be about 50% based on the relative intensity of $CH_3CH_2CO_2^-$ and $CH_3CHDCO_2^-$ ions formed via electrospray of the CH_3CHDCO_2H sample.

2.3. Mass spectrometry

Mass spectrometry experiments were conducted using a modified Finnigan LCQ quadrupole ion trap mass spectrometer equipped with a Finnigan electrospray ionisation source. Tetrabutylammonium salts of metal-oxide anions were dissolved in acetonitrile (0.1 mg/mL). The solution was pumped into the electrospray source at approximately 3 μL/min. Typical electrospray source conditions involved needle potentials of 3.5–4.0 kV and heated capillary temperatures of 150–250 °C. Extensive tuning of electrospray conditions was often required due to the low signal-to-noise ratio and/or low abundance of some species. Mass selection and collisional activation were carried out using standard isolation and excitation procedures [17] using the 'advanced scan' function of the LCQ software.

The oxo-anions species display distinctive isotope patterns due to the isotopic composition of the metals. For example, there are seven naturally occurring isotopes of molybdenum (^{92}Mo, 14.84; ^{94}Mo, 9.25; ^{95}Mo, 15.92; ^{96}Mo, 16.68; ^{97}Mo, 9.55; ^{98}Mo, 24.13; ^{100}Mo, 9.68 atom%). This facilitates assignment of ion stoichiometry via comparison of experimental and theoretical isotope patterns. However, the broad isotope pattern can also make small mass changes difficult to detect (e.g., during isotope labelling experiments involving both hydrogen and deuterium). To avoid this problem, the *single* most intense peak was mass selected from the isotope manifold, and used to follow the course of reactions. Quoted *m*/*z* values in the text refer to this most intense peak.

The instrument has been modified to permit introduction of neutral reagents into the ion trap, allowing the measurement of ion–molecule reaction rate constants [10b,18]. These modifications and the experimental procedure for measurement of ion–molecule rate constants have been described in detail previously [10b,18]. We have previously tested this procedure by comparing experimental absolute rate constants measured with the modified LCQ with literature values obtained via flowing afterglow techniques at 298 K, and have found good agreement [10b,19]. This suggests the present instrument provides ion–molecule rate constants of near thermal ions, consistent with previous rate measurements in a similar system [18] and findings that ions within the ion trap are essentially at room temperature [20].

Reaction efficiencies (ϕ) were calculated by dividing the experimentally determined rate constant (k_{exp}) by theoretical predictions of ion–molecule collision rate constants (k_{ado}); i.e., $\phi = k_{exp}/k_{ado}$. Theoretical collision rate constants were determined using the method of Su and Bowers [21].

Kinetic isotope effects for collisional activation reactions involving H transfer were determined by mass selecting a single peak of the appropriately selectively deuterated metal-acetate species and subjecting this species to collisional activation for 10 ms. The collisional activation voltage (V_{p-p}) was varied to encompass varying degrees of parent ion dissociation.

This allowed the effect of collisional activation voltage on the measured experimental KIE to be investigated.

We have also attempted to measure the threshold energies for some of the reactions of the present study that occur under collisional activation conditions. However, the estimation of absolute collision energies applied during collisional activation experiments in quadrupole ion trap instruments is not straightforward. To provide a qualitative insight into the 'critical energies' of reactions requiring collisional activation, we have compared activation voltages (V_{p-p}) required for these reaction with those required for the dissociation of two species with established critical energies, $Ag(CH_3OH)^+$ and $Fe(C_5H_5)_2{}^+$ (generated via ESI of $AgNO_3$ in CH_3OH and $Fe(C_5H_5)_2$ in CH_3CN, respectively) [22]. These species were chosen as the activation voltages required for their dissociation effectively 'brackets' the activation voltages used in present experiments.

Threshold activation voltages were determined by following the procedure of Colorado and Brodbelt [23]. A single peak from the isotope manifold of the species of interest was mass selected and an activation voltage was applied for a period of 10 ms. Activation voltages (V_{p-p}) were increased in a stepwise fashion until complete dissociation of the ion of interest was observed. The voltage at which the fragment ion intensity is 10% of the total ion intensity is defined as the 'threshold voltage'. In these experiments, a relatively low concentration of CH_3COOH (typically 1×10^{-7} Torr to 2×10^{-7} Torr) was present in the ion-trap as this neutral was required to generate the species of interest. However, it has been demonstrated previously that such low concentrations of neutral reagents in the ion trap have little effect on the measured threshold voltage [10b,23]. Given important factors such as lifetime effects, kinetic shifts, differing excitation efficiencies and mass effects have been ignored in these experiments, the data presented is only intended as a qualitative and crude estimate of the energetics of these reactions.

3. Results and discussion

3.1. Dehydration of acetic acid to ketene catalysed by $[Mo_2O_6(OH)]^-$

Negative ion electrospray mass spectrometry of $(Bu_4N)_2[Mo_2O_7]$ in acetonitrile resulted in three major products: the dimolybdate dianion, $[Mo_2O_7]^{2-}$ (*m*/*z* 152), protonated dimolybdate, $[Mo_2O_6(OH)]^-$ (*m*/*z* 305), and the ion pair, $\{Bu_4N^+[Mo_2O_7]^{2-}\}^-$ (*m*/*z* 546) [10]. Mass selection of $[Mo_2O_7]^{2-}$ and reaction with acetic acid in the gas phase resulted in proton transfer and formation of $[Mo_2O_6(OH)]^-$ (*m*/*z* 305) and the acetate anion (*m*/*z* 59) (Fig. 1, Eq. (11)).

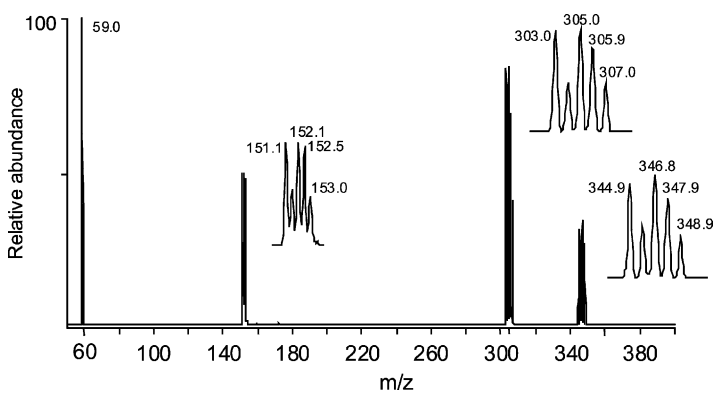

Fig. 1. Mass spectrum showing the reaction of $[Mo_2O_7]^{2-}$ (*m*/*z* 152) with CH_3COOH. Five peaks from the dimolybdate isotope manifold (see inset) were mass selected and allowed to react with CH_3COOH. Proton transfer to form $[Mo_2O_6(OH)]^-$ (*m*/*z* 305) and CH_3COO^- (*m*/*z* 59) is the only primary reaction. A secondary reaction between $[Mo_2O_6(OH)]^-$ and CH_3COOH results in elimination of water and formation of $[Mo_2O_6(OCOCH_3)]^-$ (*m*/*z* 347).

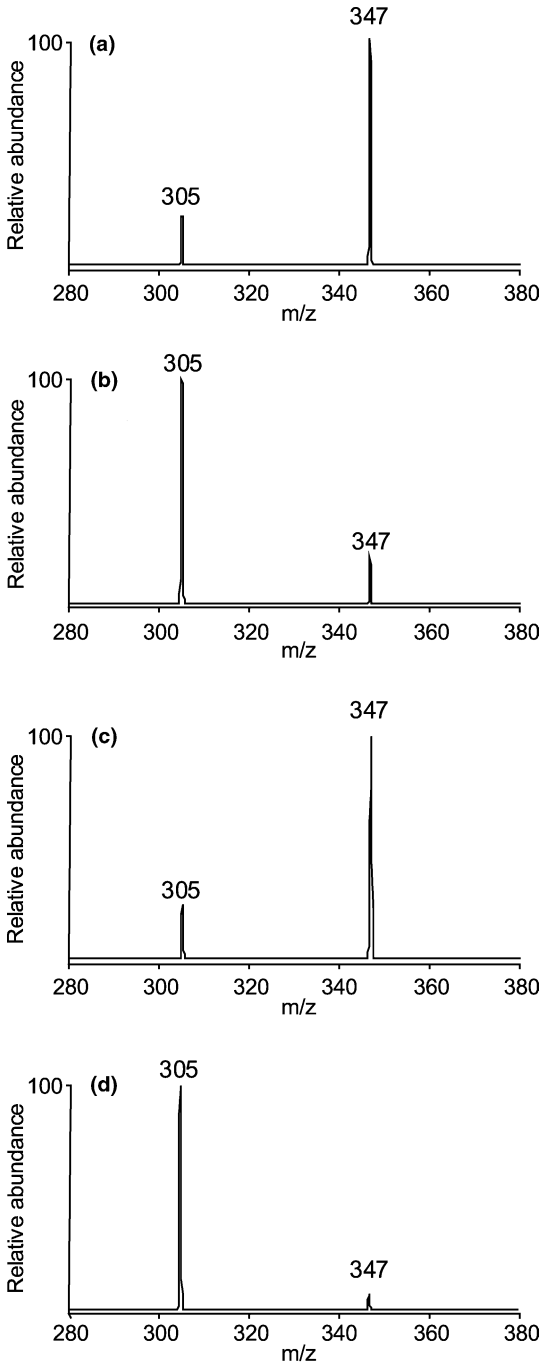

Fig. 2. Multistage mass spectrometry (MS^n) experiments illustrating the catalytic dehydration of acetic acid to ketene. A single peak (*m*/*z* 305) was mass selected from the $[Mo_2O_6(OH)]^-$ isotope manifold and followed through the relevant reactions: (a) mass selection (MS^2) of $[Mo_2O_6(OH)]^-$ (*m*/*z* 305) and reaction with acetic acid to form $[Mo_2O_6(OCOCH_3)]^-$ (*m*/*z* 347) and eliminate neutral water. (b) Mass selection (MS^3) and collisional activation of $[Mo_2O_6(OCOCH_3)]^-$ (*m*/*z* 347) to eliminate ketene and form $[Mo_2O_6(OH)]^-$ (*m*/*z* 305). (c) Mass selection (MS^4) of $[Mo_2O_6(OH)]^-$ (*m*/*z* 305) and reaction with acetic acid to form $[Mo_2O_6(OCOCH_3)]^-$ (*m*/*z* 347) and eliminate neutral water. (d) Mass selection (MS^5) and collisional activation of $[Mo_2O_6(OCOCH_3)]^-$ (*m*/*z* 347) to eliminate ketene and form $[Mo_2O_6(OH)]^-$ (*m*/*z* 305).

A further peak at *m*/*z* 347 was also apparent. Mass selection of $[Mo_2O_6(OH)]^-$ and reaction with acetic acid confirms that the peak at *m*/*z* 347 is due to a secondary reaction between the protonated dimolybdate center and acetic acid (Eq. (12), Fig. 2a). An identical reaction is observed for the equivalent protonated dimolybdate center generated directly via electrospray. This reaction is similar to that observed previously between $[M_2O_6(OH)]^-$ (M = Mo and W) and alcohols [10b]. In these experiments, isotope labelling of methanol suggested that the hydroxyl proton of methanol and the hydroxo ligand of $[M_2O_6(OH)]^-$ are lost as neutral water. Similar reactivity towards alcohols and carboxylic acids has been observed for the organometallic complex Cp_2ZrOH^+ (Cp = η^5-cyclopentadienyl) [24]. Further, this reaction is similar to that proposed to occur between CH_3COOH and M–OH units on metal-oxide surfaces (Eq. (3)) [4].

$$[Mo_2O_7]^{2-} + CH_3COOH \rightarrow [Mo_2O_6(OH)]^- + CH_3COO^- \quad (11)$$

$$[Mo_2O_6(OH)]^- + CH_3COOH \rightarrow [Mo_2O_6(OCOCH_3)]^- + H_2O \quad (12)$$

The elimination of aldehyde or ketone upon collisional activation of dimolybdate centers with primary and secondary alkoxo ligands, respectively, has been observed [10]. These reactions were proposed to occur via transfer of α-hydrogen from the alkoxo ligand to an oxo of the dimolybdate center. However, the acetate ligand of $[Mo_2O_6(OCOCH_3)]^-$ does not possess an α-hydrogen, and thus α-hydrogen transfer is not available. In a related example, collisional activation of $[Mo_2O_6(OC(CH_3)_3]^-$, which also does not

contain an α-hydrogen, resulted in the elimination of 2-methylpropene [10b]. This reaction was proposed to occur via transfer of a β-hydrogen of the tertiary alkoxo ligand to an oxo ligand of the dimolybdate center, resulting in the non-redox elimination of alkene. This suggested a similar pathway may be available for $[Mo_2O_6(OCOCH_3)]^-$.

Mass selection and collisional activation of $[Mo_2O_6(OCOCH_3)]^-$ (*m*/*z* 347) resulted solely in formation of an ion of *m*/*z* 305 (Fig. 2b). This is assigned to the elimination of neutral ketene CH_2CO (42 Da) with formation of $[Mo_2O_6(OH)]^-$ (Eq. (13)). This reaction is proposed to occur via transfer of a β-hydrogen of the acetate ligand to an oxo ligand of the dimolybdate center, a mechanism similar to that proposed for the elimination of 2-methylpropene from $[Mo_2O_6(OC(CH_3)_3]^-$ [10b]. Importantly, although decarboxylation has been observed upon collisional activation of other metal acetates in the gas phase (e.g., Eq. (14)) [25], this process was not observed for $[Mo_2O_6(OCOCH_3)]^-$.

$$[Mo_2O_6(OCOCH_3)]^- \rightarrow [Mo_2O_6(OH)]^- + CH_2CO \quad (13)$$

$$[Ag(O_2CCH_3)_2]^- \rightarrow [CH_3Ag(O_2CCH_3)]^- + CO_2 \quad (14)$$

The product of elimination of ketene from $[Mo_2O_6(OCOCH_3)]^-$ is assigned to $[Mo_2O_6(OH)]^-$. This ion corresponds to the protonated dimolybdate center whose reactivity towards acetic acid was described earlier, suggesting that this species is 'regenerated' upon elimination of ketene. Indeed, mass selection of this ion and reaction with acetic acid resulted in a reaction indistinguishable from that of the 'authentic' protonated dimolybdate, i.e., formation of $[Mo_2O_6(OCOCH_3)]^-$ and elimination of water (Fig. 2c, Eq. (12)). The product of this reaction also undergoes loss of ketene under collisional activation (Fig. 2d, Eq. (13)). These observations established these two reactions as a two-step catalytic cycle for the dehydration of acetic acid to ketene (Fig. 3). Using the multistage trapping capabilities of the ion trap instrument, it was possible to establish the cycle as truly catalytic by carrying out the two reactions five times on the same population of starting ions, an MS^{10} experiment (data not shown). By monitoring the reduction in intensity of the catalytic ion $[Mo_2O_6(OH)]^-$ it was possible to approximately evaluate the amount of this ion lost through each complete catalytic cycle. These experiments suggest that approximately 70% of the catalytic $[Mo_2O_6(OH)]^-$ ion can be 'recovered' across the two reactions of a single catalytic cycle. Given that ions are expected to be lost from the ion trap in these experiments, and that ions are also lost due to incomplete reactions, this estimate represents an absolute lower bound on the efficiency of this process.

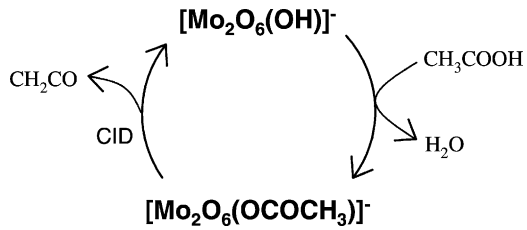

Fig. 3. Gas phase catalytic cycle for the dehydration of acetic acid to ketene.

3.2. Kinetics for the condensation of acetic acid at $[MO_3(OH)]^-$ and $[M_2O_6(OH)]^-$ centers

In order to gain further insights into the condensation reaction between $[Mo_2O_6(OH)]^-$ and CH_3COOH (Eq. (12)), we examined the reactions of all mononuclear and binuclear group VI ions, e.g., $[MO_3(OH)]^-$ and $[M_2O_6(OH)]^-$ (M = Cr, Mo, W) (Table 1). The reaction between protonated dimolybdate $[Mo_2O_6(OH)]^-$ and CH_3COOH occurred at approximately 60% of collision rate ($\phi = 0.64$). This is faster than reactions between $[Mo_2O_6(OH)]^-$ and alcohols [10b], consistent with the increased acidity of acetic acid. Protonated dichromate $[Cr_2O_6(OH)]^-$ was unreactive towards acetic acid on the timescale and concentrations of our experiments, allowing an upper bound to be placed on its reactivity ($\phi < 0.00004$). The lack of reaction between $[Cr_2O_6(OH)]^-$ and acetic acid is consistent with its lack of reactivity towards alcohols [10b]. Protonated ditungstate

Table 1
Reaction rates for reaction of mononuclear $[MO_3(OH)]^-$ and binuclear $[M_2O_6(OH)]^-$ anions (M = Cr, Mo, W) with CH_3COOH

Anion	k_{exp}[a]	k_{ado}[a,b]	Efficiency, ϕ[c]
Mononuclear			
$[CrO_3(OH)]^-$	<0.005	130	<0.00004
$[MoO_3(OH)]^-$	5.3	130	0.042
$[WO_3(OH)]^-$	0.81	120	0.0067
Binuclear			
$[Cr_2O_6(OH)]^-$	<0.005	120	<0.00004
$[Mo_2O_6(OH)]^-$	76	120	0.64
$[W_2O_6(OH)]^-$	140	120	1.20

[a] $\times 10^{-11}$ cm^3/molecules s.
[b] Theoretical collision rates, k_{ado}, are calculated using the method of Su and Bowers [21].
[c] Reaction efficiency, $\phi = k_{exp}/k_{ado}$.

$[W_2O_6(OH)]^-$ underwent an identical reaction to that observed for the molybdenum congener. However, the reaction for ditungstate was more rapid, proceeding at the collision rate. The increased reactivity of the tungsten congener over the molybdenum congener is consistent with its increased reactivity towards alcohols [10b].

The reactivity of the related mononulear $[MO_3(OH)]^-$ systems (M = Cr, Mo, W) was examined to investigate the effect of cluster size on reactivity. Protonated chromate $[CrO_3(OH)]^-$ was unreactive towards acetic acid on the timescale and concentrations of these experiments, allowing an upper bound to be placed on its gas phase reactivity ($\phi < 0.00004$). This lack of reactivity is consistent with the lack of reactivity of the related binuclear center, and the lack of reaction between $[CrO_3(OH)]^-$ and alcohols [10b]. Protonated molybdate $[MoO_3(OH)]^-$ and protonated tungstate $[WO_3(OH)]^-$ underwent analogous reactions with CH_3COOH to those observed for their binuclear counterparts, i.e., elimination of water and formation of $[MO_3(OCOCH_3)]^-$ (M = Mo, W). However, the reactivity of these mononuclear centers was diminished compared to that of their binuclear counterparts (M = Mo, $\phi = 0.042$; M = W, $\phi = 0.0067$). These mononuclear centers were unreactive towards methanol, but exhibited extremely slow reaction with the more acidic alcohol CF_3CH_2OH [10b]. The observed increase in reactivity with acetic acid is consistent with its further increase in acidity relative to alcohols.

3.3. Investigation of the elimination of ketene from $[MO_3(OCOCH_3)]^-$ and $[M_2O_6(OCOCH_3)]^-$ centers under collisional activation conditions (M = Cr, Mo, W)

We have examined the ability of the various mononuclear $[MO_3(OCOCH_3)]^-$ and binuclear $[M_2O_6(OCOCH_3)]^-$ centers (M = Cr, Mo, W) to eliminate ketene under collisional activation conditions. Given that both $[CrO_3(OH)]^-$ and $[Cr_2O_6(OH)]^-$ are unreactive towards acetic acid in the gas phase, we have not been able to generate their respective acetate species via ion–molecule reactions with acetic acid. However, these species could both be generated via electrospray of solutions of $(Bu_4N)_2[C_2O_4]$ or $(Bu_4N)_2[Cr_2O_7]$ in MeCN containing CH_3COOH (≈1% v/v). This allowed a complete comparison of the fragmentation of the mononuclear $[MO_3(OCOCH_3)]^-$ and binuclear $[M_2O_6(OCOCH_3)]^-$ species (M = Cr, Mo, W, Fig. 4).

Collisional activation of $[Cr_2O_6(OCOCH_3)]^-$ resulted in the formation of a number of product ions (Fig. 4a). While the elimination of ketene was still observed, a number of additional fragmentation pathways are also evident. Additional neutral losses of 46 = [C, H_2, O_2], 59 = [C_2, H_3, O_2], 74 = [C_2,H_2,O_3] and 101 = [Cr, O_3, H] are also observed. These neutral losses are supported by analogous experiments using labelled $[Cr_2O_6(OCOCD_3)]^-$. While we refrain from a detailed assignment of these neutral losses and a discussion of the mechanism of their formation, it is apparent that the selectivity of the dichromate center towards ketene elimination is significantly lower than that of the analogous dimolybdate center. Indeed, the elimination of ketene from $[Cr_2O_6(OCOCH_3)]^-$ (*m*/*z* 259) to form $[Cr_2O_6(OH)]^-$ (*m*/*z* 217) represents a very minor channel only (cf., the sole neutral loss from $[Mo_2O_6(OCOCH_3)]^-$ is ketene, Fig. 4b). The observed lack of selectivity for the dichromate center is consistent with its stronger oxidising power relative to the dimolybdate center.

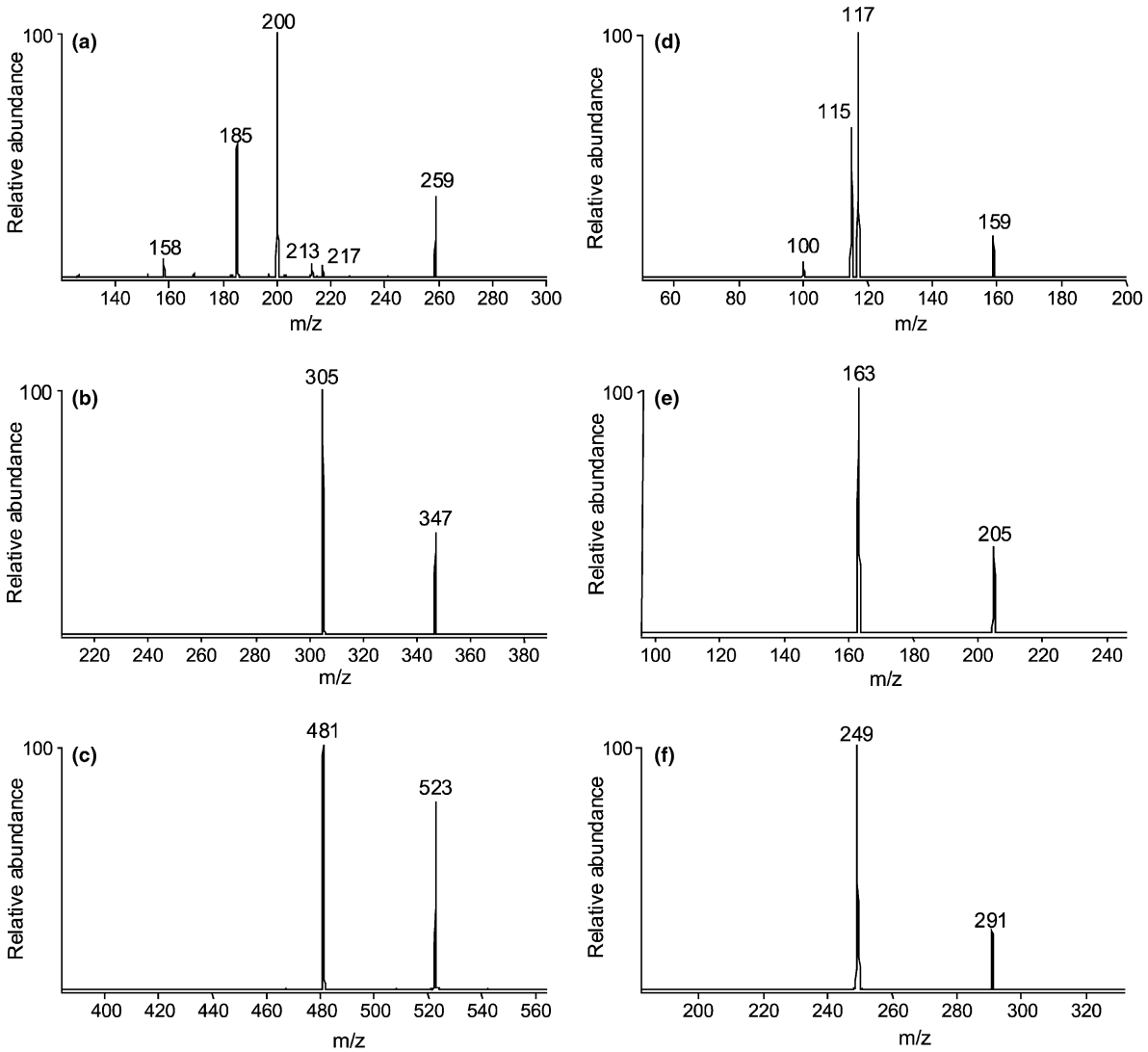

Fig. 4. Collisional activation of $[MO_3(OCOCH_3)]^-$ and $[M_2O_6(OCOCH_3)]^-$ centres (M = Cr, Mo, W). Collisional activation of: (a) $[Cr_2O_6(OCOCH_3)]^-$ (*m*/*z* 259) resulted in elimination of a variety of neutral products (see text). Importantly, the elimination of ketene to form $[Cr_2O_6(OH)]^-$ (*m*/*z* 217) is a very minor channel only. (b) $[Mo_2O_6(OCOCH_3)]^-$ (*m*/*z* 347) solely resulted in elimination of ketene to form $[Mo_2O_6(OH)]^-$ (*m*/*z* 305). (c) $[W_2O_6(OCOCH_3)]^-$ (*m*/*z* 523) solely resulted in elimination of ketene to form $[W_2O_6(OH)]^-$ (*m*/*z* 481). (d) $[CrO_3(OCOCH_3)]^-$ (*m*/*z* 159) resulted in elimination of ketene to form $[CrO_3(OH)]^-$ (*m*/*z* 117) and CO_2 to form [Cr, O_3, C, H_3]$^-$ (*m*/*z* 115). The peak at *m*/*z* 100 is the result of further fragmentation of [Cr, O_3, C, H_3]$^-$. (e) $[MoO_3(OCOCH_3)]^-$ (*m*/*z* 205) solely resulted in elimination of ketene to form $[MoO_3(OH)]^-$ (*m*/*z* 163). (f) $[WO_3(OCOCH_3)]^-$ (*m*/*z* 291) solely resulted in elimination of ketene to form $[WO_3(OH)]^-$ (*m*/*z* 249).

Collisional activation of $[W_2O_6(OCOCH_3)]^-$ resulted in the elimination of ketene (Fig. 4c), the equivalent reaction to that observed for $[Mo_2O_6(OCOCH_3)]^-$ (Fig. 4b). This is consistent with the weaker oxidizing power of W(VI) centres, and is also consistent with the preference for $[W_2O_6(OCH_2CH_3)]^-$ to undergo elimination of ethene via a related β-hydrogen transfer [10b]. The elimination

of ketene from $[W_2O_6(OCOCH_3)]^-$ established an identical catalytic cycle for the binuclear tungsten system $[W_2O_6(OH)]^-$ to that shown in Fig. 3 for $[Mo_2O_6(OH)]^-$.

We have also examined the fragmentation of mononuclear $[MO_3(OCOCH_3)]^-$ centers (M = Cr, Mo, W). Collisional activation of $[CrO_3(OCOCH_3)]^-$ resulted in neutral losses of 42 and 44 Da, to form ions of *m*/*z* 117 and 115 (Fig. 4d). This is assigned to the loss of neutral CH_2CO and CO_2, respectively. The fragmentation of $[CrO_3(OCOCH_3)]^-$ is considerably less complicated than its binuclear counterpart, $[Cr_2O_6(OCOCH_3)]^-$. Two important differences are apparent: (i) the elimination of ketene represents the major reaction channel for the mononuclear center, and a minor channel only for the binuclear center; and (ii) decarboxylation is the only fragmentation pathway in competition with ketene elimination for the mononuclear center, while a variety of other pathways are apparent for the binuclear center. These differences highlight the importance of the size ('nuclearity') of the cluster in determining its fragmentation pathways. Evidently, the presence of a neighbouring CrO_3 unit in binuclear $[Cr_2O_6(OCOCH_3)]^-$ introduces additional fragmentation pathways that are not available to mononuclear $[CrO_3(OCOCH_3)]^-$. This is consistent with differences observed previously for the fragmentation of mononuclear $[MoO_3(OCH_2CH_3)]^-$ (eliminated CH_2CH_2) and binuclear $[Mo_2O_6(OCH_2CH_3)]^-$ (eliminated CH_3CHO) [10b].

Both the mononuclear molybdenum and tungsten centers $[MO_3(OCOCH_3)]^-$ also exclusively eliminated ketene to regenerate $[MO_3(OH)]^-$ (M = Mo, W) (Fig. 4e and f). These reactions establish identical catalytic cycles to Fig. 3 for the mononuclear molybdenum and tungsten centers.

The kinetic isotope effect for the elimination of methylketene from mononuclear $[MoO_3(OCOCH_2CH_3)]^-$ and binuclear $[M_2O_6(OCOCH_2CH_3)]^-$ (M = Mo, W) centers was examined via collisional activation of species containing a selectively labelled acetate ligand. Collisional activation of $[Mo_2O_6(OCOCHDCH_3)]^-$ resulted in the elimination of $(CH_3)HCCO$ and $(CH_3)DCCO$ (Fig. 5). The

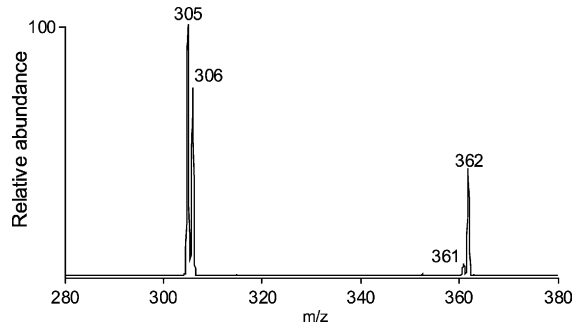

Fig. 5. Collisional activation of $[Mo_2O_6(OCOCHDCH_3)]^-$ (*m*/*z* 362) to eliminate CH_3CDCO and form $[Mo_2O_6(OH)]^-$ (*m*/*z* 305) or CH_3CHCO and form $[Mo_2O_6(OD)]^-$ (*m*/*z* 306). The peak at *m*/*z* 361 is from ensuing reaction of the product ions $[Mo_2O_6(OH)]^-$ (*m*/*z* 305) and $[Mo_2O_6(OD)]^-$ (*m*/*z* 306) with CH_3CH_2COOH impurity in the $CH_3CHDCOOH$ sample.

ratio of the neutral losses $(CH_3)DCCO$:$(CH_3)HCCO$ (inferred from the ratio of the resultant product anions, $[Mo_2O_6(OH)]^-$ and $[Mo_2O_6(OD)]^-$, respectively) defines the KIE for this reaction. Given that this reaction only occurs under collisional activation conditions, any isotope effects inferred from these experiments are only intended to reflect the KIE under the collisional activation conditions of the present experiments.

Based on experiments using collisional activation conditions where greater than 20% parent ion dissociation has occurred, a KIE for the elimination of $(CH_3)HCCO$ from $[Mo_2O_6(OCOCH_2CH_3)]^-$ in the range of 1.3–1.5 was inferred. This estimate is slightly lower than a previous estimate of 1.9 ± 0.4 for the oxidation and elimination of the ethoxo ligand in $[Mo_2O_6(OCH_2CH_3)]^-$ as acetaldehyde [10b].

We have also carried out identical experiments for the elimination of $(CH_3)HCCO$ from the related binuclear ditungstate center $[W_2O_6(OCOCH_2CH_3)]^-$ and mononuclear molybdate center $[MoO_3(OCOCH_2CH_3)]^-$. A similar kinetic isotope effect in the range of 1.4–1.6 was found for the elimination of $(CH_3)HCCO$ from the related binuclear ditungstate center $[W_2O_6(OCOCH_2CH_3)]^-$. Similarly, a range of 1.5–1.8 was estimated for the related mononuclear molybdenum counterpart $[MoO_3(OCOCH_2CH_3)]^-$.

These experiments suggest that the kinetic isotope effect for this reaction is very similar for mononuclear $[MoO_3(OCOCH_2CH_3)]^-$ and binuclear $[M_2O_6(OCH_2CH_3)]^-$ (M = Mo and W) centres, suggesting that the KIE for this reaction is relatively insensitive to changes in metal (Mo or W) or size of the cluster (mononuclear or binuclear).

To provide qualitative insights into the energetics of elimination of ketene from $[Mo_2O_6(OCOCH_3)]^-$, we have compared the collisional activation voltages required for this reaction to those required for two reactions with well defined critical energies (Fig. 6). The critical energy for dissociation of $Ag(CH_3OH)^+$ is 33 ± 3.7 kcal/mol (Fig. 6, threshold voltage = $0.38\,V_{p-p}$) and the critical energy for dissociation of $Fe(C_5H_5)_2{}^+$ is 85 ± 7 kcal/mol (Fig. 6, threshold voltage = $0.94\,V_{p-p}$) [22]. The threshold voltages required for these reactions effectively 'bracket' the threshold voltage required for elimination of ketene from $[Mo_2O_6(OCOCH_3)]^-$ (Fig. 6, threshold voltage = $0.61\,V_{p-p}$). This suggests a crude estimate for the elimination of ketene from $[Mo_2O_6(OCOCH_3)]^-$ as 55 ± 20 kcal/mol. This estimate is only slightly lower (approx. 10–18 kcal/mol) than estimates for the unimolecular decomposition of acetic acid to ketene [3]. However, given that the elimination of ketene from $[Mo_2O_6(OCOCH_3)]^-$ requires less energy than the unimolecular decomposition of acetic acid to ketene, it is appropriate to call the catalytic cycle of Fig. 3 'truly catalytic' for the dehydration of acetic acid to ketene. Furthermore, while the unimolecular decomposition of acetic acid also produces methane and CO_2 (Eq. (2)), the process catalysed by $[Mo_2O_6(OH)]^-$ produces only ketene and water.

For comparative purposes, we have also measured the threshold activation voltages required for the elimination of ketene from the related mononuclear molybdate $[MoO_3(OCOCH_3)]^-$ and binuclear ditungstate $[W_2O_6(OCOCH_3)]^-$ centers. The threshold voltage for elimination of ketene from $[MoO_3(OCOCH_3)]^-$ is $0.56\,V_{p-p}$. This is only slightly lower than that required for the binuclear dimolybdate center. The threshold voltage for elimination of ketene from $[W_2O_6(OCOCH_3)]^-$ is $0.75\,V_{p-p}$, only slightly higher than that required for the related molybdenum species. Given the different masses and sizes of these three clusters, it is difficult to quantitatively compare the threshold voltages required for the elimination of ketene. However, these experiments indicate that the size of the cluster and the metal of the cluster appears to have little effect on the energy required for the elimination of ketene. This is consistent with the earlier observation that the kinetic isotope effect

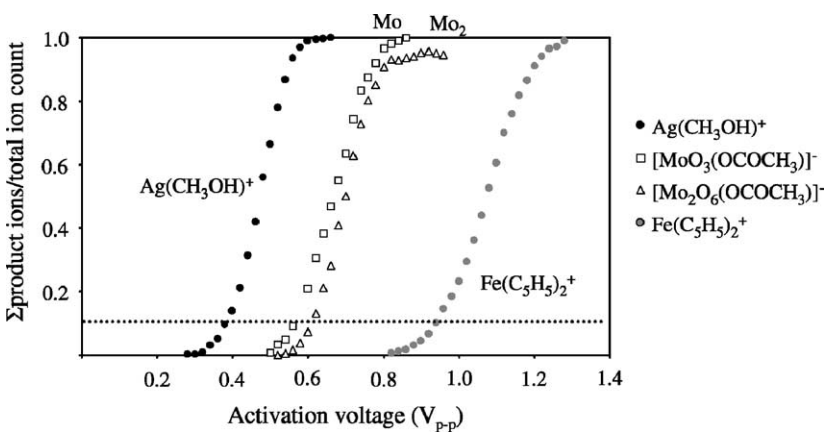

Fig. 6. Plot of reaction extent (Σproduct ions/total ion count) vs. activation voltage (V_{p-p}) for elimination of CH_2CO from $[MO_3(OCOCH_3)]^-$ and $[Mo_2O_6(OCOCH_3)]^-$. The critical energies for dissociation of $Ag(CH_3OH)^+$ (33.0 ± 3.7 kcal/mol) and $Fe(C_5H_5)_2{}^+$ (85 ± 7 kcal/mol) are known [22]. The dashed line corresponds to 10% reaction extent, the point at which threshold activation voltages are measured.

for elimination of methylketene was also relatively insensitive to these factors.

3.4. Discussion of the gas phase catalytic cycle and its relationship to condensed phase catalysts

Barteau and co-workers have proposed the following properties for metal oxide surface sites to promote ketene formation from carboxylic acids [4]: (i) exposed surface cations must be coordinatively unsaturated in order to dissociate the acid; (ii) unimolecular decomposition of absorbed carboxylate to form ketene occurs at cations with a single coordination vacancy; and (iii) selectivity for ketene production is higher for oxides that are difficult to reduce (reducible oxides tend to produce CO_2 by decarboxylation). Of these requirements, the latter is of most interest relative to the results of this study. While both mononuclear and binuclear molybdenum and tungsten systems cleanly expel ketene, the chromium analogues undergo a variety of neutral losses, including decarboxylation and other neutral losses that presumably result in reduction of the metal-oxo center. This contrasting behaviour is consistent with the expected stronger oxidizing power of chromium compared to that of molybdenum and tungsten species [26], and with the proposals of Barteau and co-workers [4].

For catalytic ketene formation, the metal species must be regenerated and the energetic requirements for ketene formation must be lowered. Regarding the latter point, recent high level ab initio calculations have revealed that the one step mechanism for elimination of water from acetic acid to form ketene proceeds via a high energy (71 kcal/mol) 1,2-elimination involving the four-centered transition state **A** [3]. In contrast, metal-oxo species may catalyse the elimination of ketene via a two step process (e.g., Eqs. (3) and (4) or Eqs. (12) and (13)). In the second step (Eqs. (4) or (13)), transition states which involve more atoms (i.e., larger rings) may lower the barrier for ketene elimination through the involvement of an adjacent oxo ligand (e.g., **B**). An estimate of 55 ± 20 kcal/mol for the critical energy for elimination of ketene from $[Mo_2O_6(OCOCH_3)]^-$ was derived in the present study. This is consistent with a previous estimate based on temperature-programmed desorption experiments of 50 kcal/mol for the activation energy for the dehydration of acetic acid to ketene on silica surfaces [4a]. Both of these estimates are less than the energy required for the unimolecular decomposition of acetic acid to ketene, estimated to be in the range of 65–73 kcal/mol [3].

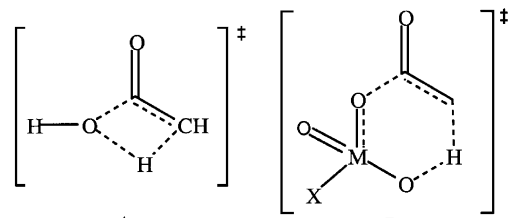

A **B**

4. Conclusions

A two step gas phase catalytic cycle is presented for the dehydration of acetic acid to ketene with the binuclear dimolybdate center $[Mo_2O_6(OH)]^-$ acting as the catalyst (Fig. 3). The first step involves condensation with acetic acid to yield the acetate complex $[Mo_2O_6(OCOCH_3)]^-$. The second step involves elimination of ketene under conditions of collisional activation to reform $[Mo_2O_6(OH)]^-$. The nature of these reactions was probed by kinetic measurements, by isotope labelling and by variation of the reactive center (metal and nuclearity). The molybdenum and tungsten mononuclear $[MO_3(OH)]^-$ and binuclear centers $[M_2O_6(OH)]^-$) (M = Mo, W) promoted reaction (1) but the chromium centers $[CrO_3(OH)]^-$ and $[Cr_2O_6(OH)]^-$) did not (Table 1). This is consistent with the expected order of basicity of the hydroxo ligand in these species and with previous studies on the reactivity of the same anions towards alcohols [10b]. Collisional activation of mononuclear $[MO_3(OCOCH_3)]^-$ and binuclear $[M_2O_6(OCOCH_3)]^-$ molybdenum and tungsten systems (M = Mo, W) resulted in the elimination of ketene. In contrast, the analogous chromium systems $[CrO_3(OCOCH_3)]^-$ and $[Cr_2O_6(OCOCH_3)]^-$ were

considerably less selective for elimination of ketene, and underwent a variety of different fragmentation channels, including redox reactions. This is consistent with the expected order of oxidizing power of the anions. The two reactions which constitute the catalytic cycle of Fig. 3 are equivalent to the two essential steps proposed to occur for the dehydration of acetic acid over metal oxide and silica surfaces [4].

Acknowledgements

T.W. acknowledges the support of an Australian Postgraduate Award. T.W. and R.A.J.O. thank Professor Scott Gronert helpful discussions concerning rate measurements. R.A.J.O. thanks the Australian Research Council for financial support (grant #A00103008), the University of Melbourne for funds to purchase the LCQ.

References

[1] C. Abaecherli, R.J. Miller, Ketenes, ketene dimers and related substances, in: J.I. Kroschwitz, M. Howe-Grant (Eds.), Kirk-Othmer Encyclopedia of Chemical Technology, 4th ed., vol. 14, Wiley, New York, 1995, p. 954.
[2] T.T. Tidwell, Ketenes, Wiley, New York, 1995.
[3] W.-H. Fang, R.-Z. Liu, X. Zheng, D.L. Phillips, J. Org. Chem. 67 (2002) 8407, and references cited therein.
[4] (a) M.C. Libby, P.C. Watson, M.A. Barteau, Ind. Eng. Chem. Res. 33 (1994) 2904;
(b) M.A. Barteau, Chem. Rev. 96 (1996) 1413.
[5] (a) K.J. Fisher, Prog. Inorg. Chem. 50 (2001) 343;
(b) K. Eller, H. Schwarz, Chem. Rev. 91 (1991) 1121;
(c) K. Eller, Coord. Chem. Rev. 126 (1993) 93;
(d) B.S. Freiser, J. Mass Spectrom. 31 (1996) 703;
(e) D. Schröder, H. Schwarz, Angew Chem. Int. Ed. Engl. 34 (1995) 1973;
(f) D. Schröder, H. Schwarz, S. Shaik, Struct. Bond. 97 (2000) 91;
(g) P.B. Armentrout, Ann. Rev. Phys. Chem. 52 (2001) 423;
(h) I. Kretzschmar, D. Schröder, H. Schwarz, P.B. Armentrout, in: M.A. Duncan (Ed.), Adv. Met. Semicond. Clust. 5 (2001) 347;
(i) P.B. Armentrout, in: J.M. Brown, P. Hofmann (Eds.), Topics in Organometallic Chemistry, vol. 4, Springer-Verlag, Berlin, 1999, p. 1;
(j) P.B. Armentrout, J.B. Griffin, J. Conceição, in: G.N. Chuev, V.D. Lakhno, A.P. Nefedov (Eds.), Progress in Physics of Clusters, World Scientific, Singapore, 1999, p. 198;
(k) D.H. Russell (Ed.), Gas Phase Inorganic Chemistry, Plenum Press, New York, 1989.
[6] (a) M. Lombarski, J. Allison, Int. J. Mass Spectrom. Ion Process. 65 (1985) 31;
(b) D. Schröder, W. Zummack, H. Schwarz, J. Am. Chem. Soc. 116 (1994) 5857;
(c) D. Schröder, A. Fiedler, J. Hrusak, H. Schwarz, J. Am. Chem. Soc. 114 (1992) 1215;
(d) R.C. Burnier, G.D. Byrd, B.S. Freiser, Anal. Chem. 52 (1980) 1641.
[7] (a) Homogeneous Catalysis—Quo vadis? W.A. Herrmann, B. Cornils, in: W.A. Herrmann, B. Cornils (Eds.), Applied Homogeneous Catalysis with Organometallic Compounds, vol. 2, VCH, Weinheim, 1996, Chapter 4, p. 1179;
(b) D.A. Plattner, Int. J. Mass Spectrom. 207 (2001) 125;
(c) K.A. Zemski, D.R. Justes, A.W. Castleman Jr., J. Phys. Chem. B 106 (2002) 6136.
[8] (a) M.M. Kappes, R.H. Staley, J. Am. Chem. Soc. 103 (1981) 1286;
(b) V. Boranov, G. Javahery, A.C. Hopkinson, D.K. Bohme, J. Am. Chem. Soc. 117 (1995) 12801;
(c) Y. Shi, K.M. Ervin, J. Chem. Phys. 108 (1998) 1757;
(d) P. Schnabel, M.P. Irion, K.G. Weil, J. Phys. Chem. 95 (1991) 9688.
[9] (a) D. Schröder, H. Schwarz, Angew Chem. Int. Ed. Engl. 29 (1990) 1433;
(b) D. Schröder, H. Schwarz, Angew Chem. Int. Ed. Engl. 29 (1990) 1431;
(c) R. Wesendrup, D. Schröder, H. Schwarz, Angew Chem. Int. Ed. Engl. 33 (1994) 1174;
(d) C. Heinemann, R. Wesendrup, H. Schwarz, Chem. Phys. Lett. 239 (1995) 75;
(e) M. Pavlov, M.R.A. Blomberg, P.E.M. Siegbahn, R. Wesendrup, C. Heinemann, H. Schwarz, J. Phys. Chem. A 101 (1997) 1567.
[10] (a) T. Waters, R.A.J. O'Hair, A.G. Wedd, Chem. Commun. (2000) 225;
(b) T. Waters, R.A.J. O'Hair, A.G. Wedd, J. Am. Chem. Soc. 125 (2003) 3384.
[11] D. Landini, F. Rolla, Chem. Ind. 6 (1979) 213.
[12] N.H. Hur, W.G. Klemperer, R.-C. Wang, Inorg. Synth. 27 (1990) 79.
[13] H. Nakayama, Bull. Chem. Soc. Jpn. 56 (1983) 877.
[14] W.G. Klemperer, R.-S. Liu, Inorg. Chem. 19 (1980) 3863.
[15] T.M. Che, V.W. Day, L.C. Francesconi, M.F. Fredrich, W.G. Klemperer, W. Shum, Inorg. Chem. 24 (1985) 4055.
[16] M.S. Matta, D.E. Broadway, M.K. Stroot, J. Am. Chem. Soc. 109 (1987) 4916.
[17] R.E. March, J.F.J. Todd (Eds.), Practical Aspects of Ion Trap Mass Spectrometry, CRC Press, Florida, 1995;
(a) Fundamentals of Ion Trap Mass Spectrometry, vol. 1;
(b) Ion Trap Instrumentation, vol. 2.
[18] (a) A.E. Flores, S. Gronert, J. Am. Chem. Soc. 121 (1999) 2627;
(b) S. Gronert, J. Am. Chem. Soc. 123 (2001) 3081.
[19] S. Gronert, C.H. DePuy, V.M. Bierbaum, J. Am. Chem. Soc. 113 (1991) 4009.

[20] S. Gronert, J. Am. Soc. Mass Spectrom. 9 (1998) 845.
[21] T. Su, M.T. Bowers, in: M.T. Bowers (Ed.), Gas-Phase Ion Chemistry, Academic Press, New York, 1979, p. 83.
[22] (a) $Ag(CH_3OH)^+ \rightarrow Ag^+ + CH_3OH$, see H. El Aribi, T. Shoeib, Y. Ling, C.F. Rodriquez, A.C. Hopkinson, K.W.M. Siu, J. Phys. Chem. A 106 (2002) 2908;
(b) $Fe(C_5H_5)_2{}^+ \rightarrow Fe(C_5H_5)^+ + C_5H_5^{\bullet}$, see J.D. Faulk, R.C. Dunbar, J. Am. Chem. Soc. 114 (1992) 8596.
[23] A. Colorado, J. Brodbelt, J. Am. Soc. Mass Spectrom. 7 (1996) 1116.
[24] D.E. Richardson, G.H.L. Lang, E. Crestoni, M.F. Ryan, J.E. Eyler, Int. J. Mass Spectrom. 204 (2001) 255.
[25] R.A.J. O'Hair, Chem. Commun. (2002) 20.
[26] (a) S. Brownstein, G.A. Heath, A. Sengupta, D.W.A. Sharp, Chem. Commun. (1983) 669;
(b) G.A. Heath, K.A. Moock, D.W.A. Sharp, L.J. Yellowlees, Chem. Commun. (1985) 1503.